



## Electrochemical Generation of Ozone in a Membrane Electrode Assembly Cell with Convective Flow

Yuhong Cui,<sup>a,b,c</sup> Yunhai Wang,<sup>a,d</sup> Bin Wang,<sup>a,\*</sup> Haihui Zhou,<sup>a</sup>  
Kwong-Yu Chan,<sup>a,\*\*,z</sup> and Xiao-Yan Li<sup>b</sup>

<sup>a</sup>Department of Chemistry, and <sup>b</sup>Department of Civil Engineering, The University of Hong Kong, Hong Kong SAR, China

Highly efficient electrochemical generation of ozone on doped tin dioxide anodes was reported recently. Here, we report the scale up of such ozone generation on a membrane electrode assembly (MEA) made with  $8 \times 13$  cm-doped tin dioxide anode. The effects of water flow rate, operating voltage, and current on dissolved ozone concentration, ozone production, current efficiency, and energy efficiency are reported. Ozone production and current efficiency increased with water flow. Operating with a single MEA, 218 mg/h of dissolved ozone was produced at an applied current of 6 A (current density =  $57.6 \text{ mA/cm}^2$ ). With four MEAs operated in a stack, the dissolved ozone production increased to 1.1 g/h at a total current of 20.6 A (current density =  $49.5 \text{ mA/cm}^2$ ) and individual cell voltage of 3.3 V. For the multiple MEA operation, the highest current efficiency was 21.7% based alone on dissolved ozone generation. The lowest energy consumption achieved was 42 kWh/kg ( $\text{O}_3$ ) at 643 mg ozone per hour at current of 10.1 A (current density =  $24.3 \text{ mA/cm}^2$ ) and water flow of 5.4 L/min (linear velocity = 7.03 cm/s). © 2009 The Electrochemical Society. [DOI: 10.1149/1.3072686] All rights reserved.

Manuscript submitted August 8, 2008; revised manuscript received December 7, 2008. Published January 30, 2009.

Ozone has broad applications in disinfection, bleaching, water treatment, wastewater treatment, environmental cleanup, and chemical synthesis. The oxidation potential of ozone is 2.07 V, higher than that of most common oxidizing chemicals, such as chlorine.<sup>1</sup> As a powerful oxidant, ozone can rapidly remove a large variety of organic pollutants and persistent pathogens. More importantly, there is no harmful by-product or no residual effects as ozone decomposes into oxygen with time. However, this property makes ozone difficult to be stored. Ozone must be generated and applied in situ. Ozone is conventionally synthesized through high voltage cold corona discharge (CCD), producing a 2–3% concentration of ozone<sup>2</sup> from air. The overall energy consumption of the CCD process is high because cooling and drying of air are needed in addition to high voltage. The CCD process can produce nitrogen oxide ( $\text{NO}_x$ ) as a by-product unless nitrogen is removed by additional energy. The energy required to purify air to oxygen is at least two times that of making ozone from oxygen.<sup>3</sup> An alternative generation method is via UV radiation at 185 nm. However, the generated ozone concentration is lower than that of CCD production and more electrical energy is consumed. UV lamps also need periodic replacement with additional expenses. Electrochemical ozone generation in liquid phase is an attractive alternative. It does not require high voltage to ionize gaseous oxygen molecules and a few volts of dc source are sufficient for ozone generation in an electrolyte. Water electrolysis in a low-voltage condition eliminates any possibility of  $\text{NO}_x$  formation. If dissolved ozone is the desired product, then the water electrolysis route is more direct and effective. The decay and loss during transfer from gaseous ozone to dissolved ozone are avoided.

The electrochemical synthesis of ozone was investigated in the early 1980s and was reviewed recently.<sup>4,5</sup> The effectiveness of electrolytic ozone generation depends critically on electrode materials and the reactor design. A number of anode materials have been examined previously for the electrochemical ozone generation, but low efficiency has been demonstrated for most electrodes.<sup>6–12</sup> Lead dioxide has been the most investigated anode material with considerable effectiveness, but is environmentally prohibitive for a general usage. A very high efficiency of 47% on electrochemical ozone production has been reported by using boron-doped diamond electrode

materials with an effective anode area of  $1.5 \times 5 \text{ cm}$ .<sup>13</sup> High concentration of ozone and high current efficiency were also achieved with doped tin dioxide electrode recently.<sup>14,15</sup> Acid electrolytes are usually adopted to investigate performance of electrochemical ozone production. For corrosion and safety consideration, it will be desirable to have an acid-free process in practical ozone generation, particularly for domestic household applications. Furthermore, hydrogen generated at the cathode during electrolysis creates a safety concern. These problems can be circumvented by the use of a water-filled polymer electrolyte membrane (PEM) cell fitted with an air cathode, as reported recently.<sup>16</sup> The ozone concentrations reported with doped tin oxide anodes are much higher than the CCD process.

Our previous work on a membrane electrode assembly (MEA) using pure water was on a  $4 \times 6$  cm-doped tin oxide anode without convection.<sup>16</sup> In studies of electrochemical generation of ozone on  $\text{PbO}_2$  anode, efficiency increased with flow of electrolyte using either water or 0.001 M  $\text{Na}_2\text{SO}_4$  as electrolyte.<sup>17,18</sup> Here, we investigate convection effects and the scale-up effect in a design using large  $8 \times 13$  cm MEAs. An ozone production rate at 1.1 g/h was achieved with a four-MEA stack running with water, demonstrating the practicality of the doped oxide anode technology for small ozone generation units. In the following sections, the experimental setup, effects of flow rate and current (voltage) on ozone concentration, ozone production, and current efficiency are discussed.

### Experimental

**Preparation of electrode and MEA.**—The components and operation of the MEA are shown schematically in Fig. 1a. A mesh anode coated with doped  $\text{SnO}_2$  was hot pressed to a Nafion PEM together with an air diffusion cathode.

The anode was prepared by the repeated procedure of coating wet metal precursors onto a titanium substrate and firing the coated substrate in air oven as previously described.<sup>14–16,19</sup> An  $8 \times 13$  cm titanium mesh (Dexmet Corporation, 5 Ti 5-031), 0.127 mm thick with a nominal aperture of 0.787 mm, wire strand width of 0.127 mm was used as the substrate. The mesh was then rinsed with acetone, treated in 10% boiling oxalic acid for 1 h, washed with deionized water, and dried. Different from the previous procedure,<sup>14–16,19</sup> which had the potential of oxidizing the titanium substrate in the first firing, electrodeposition of the antimony-tin layer was applied first. For electrodeposition, the pretreated Ti mesh was placed as the cathode in 500 mL of alcohol solution containing 43.75 g  $\text{SnCl}_4 \cdot 5\text{H}_2\text{O}$  (98%, ABCR), 1.395 g  $\text{SbCl}_3$  (BDH, 99.5%). The deposition procedure was 1 A (current density =  $4.8 \text{ mA/cm}^2$ ) for 1 min followed by 0.5 A (current density =  $2.4 \text{ mA/cm}^2$ ) for 20 min in a three-chamber cell with two counter electrodes made of

\* Electrochemical Society Student Member.

\*\* Electrochemical Society Active Member.

<sup>c</sup> Present address: School of Environmental Science and Engineering, Huazhong University of Science and Technology, Wuhan 430074, China.

<sup>d</sup> Present address: Department of Environmental Science and Engineering, Faculty of Energy and Power, Xi'an Jiaotong University, Xi'an, 710049, China.

<sup>z</sup> E-mail: hrsceky@hku.hk

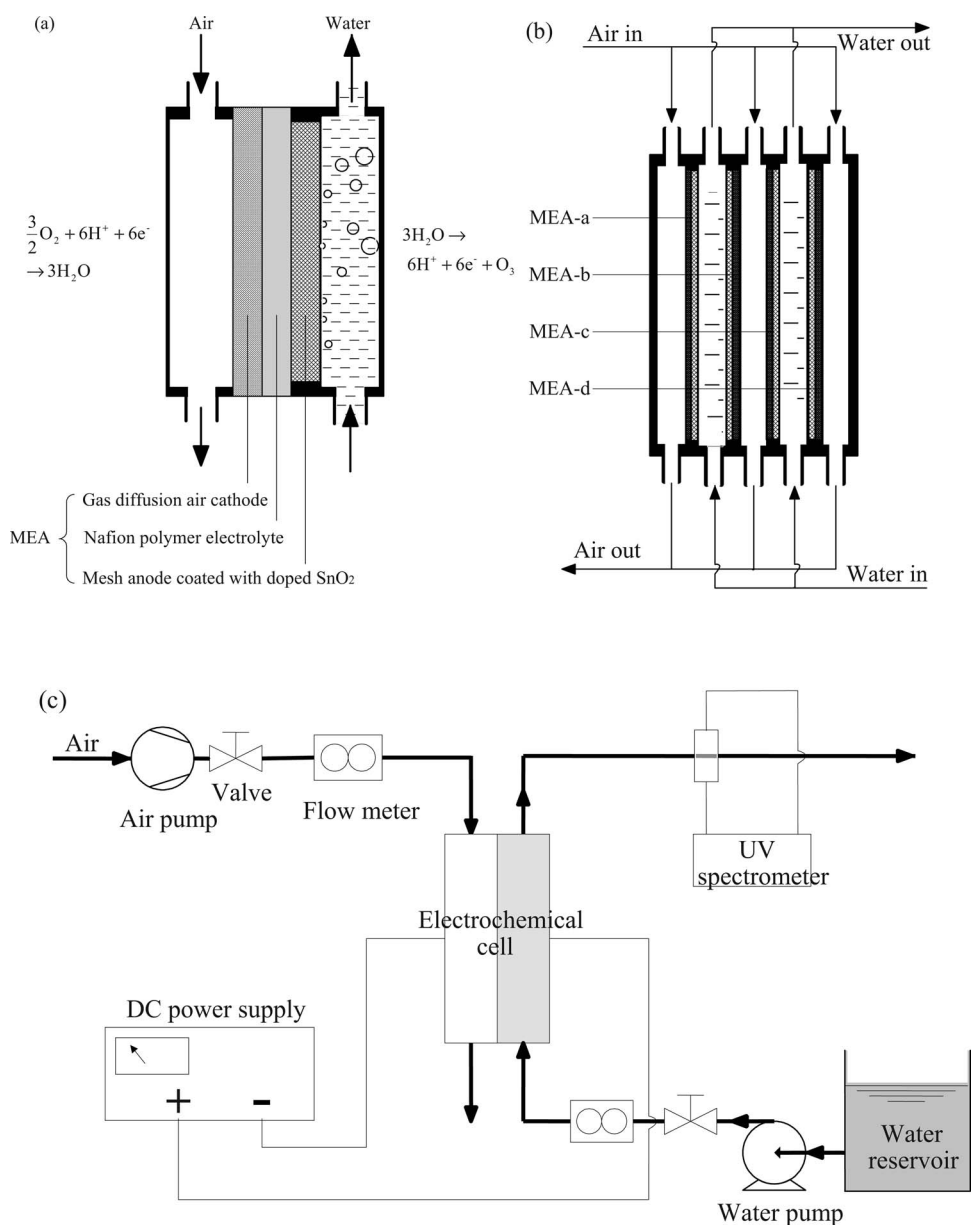


**Figure 1.** Schematic of (a) the operation of a single MEA, (b) flow distribution in four MEA stack, and (c) the flow system for ozone production and on-line measurements of dissolved ozone.

platinized Ti meshes. After electrodeposition, the mesh was heated in an oven at 390°C for 1 h. From the second coating step onward, the mesh was fired after being dip coated in an alcohol solution consisting of 140.00 g SnCl<sub>4</sub>·5H<sub>2</sub>O (98%, ABCR), 1.43 g SbCl<sub>3</sub> (BDH, 99.5%), and 0.1854 g NiCl<sub>2</sub>·6H<sub>2</sub>O (Merck, 98%) in 400 mL n-butanol. The coating was repeated 15 times each with a cycle of dip coating, 5 min preheating followed by 10 min pyrolysis at 390°C. In the last cycle, the pyrolysis step was carried out at 420°C for 1 h.

The cathode was prepared by pasting 50% Pt/C catalyst (De Nora North America, ETEK Division) onto one side of a 10 × 15 cm carbon cloth (ETEK, 50% wet proofed). The platinum loading on the cathode was 5 mg/cm<sup>2</sup>. The MEA was prepared by hot pressing air cathode, a solid electrolyte Nafion 117 membrane wetted on both sides with 5% Nafion solution (Fuel Cell Scientific), and the doped SnO<sub>2</sub> anode with a force of 3000 N at 135°C for 3 min.

*Setup of electrochemical experiment and ozone measurement.*—The experimental setup and flow arrangements of single and multiple MEAs in a stack are shown in Fig. 1. The compartment ele-

ments for the single-cell experiment and the stack experiment are the same but configured differently and with a different number of pieces. The chamber is formed by a separating plate between two MEAs (Fig. 1b) or between the MEA and the ending plate (Fig. 1a) with ribs partitioning the cavity into vertical channels for water (or air) flow over the electrodes. Both anode and cathode chambers have internal dimensions of 13 × 8 cm and 0.8 mm thick. Without considering the volume of supporting ribs in the cavity, the liquid/air holdup volume can be estimated to be ~83 mL (8 × 13 × 0.8 cm). The linear velocities at different water flow rates are calculated using this nominal volume. In the multiple-MEA stack experiment, though two MEA anodes share the same cavity, the linear velocity of water over each anode is the same in the case of a single MEA configuration with identical flow per channel. Results presented here are mostly for operation with one MEA. Milli-Q water of 20°C with electrical resistance of 18.2 MΩ cm was pumped into the anodic chamber at a fixed flow rate. The cathode can be running with either passive air breathing or forced airflow at 10 L/min (nominal linear velocity = 26.04 cm/s). Oxygen from air

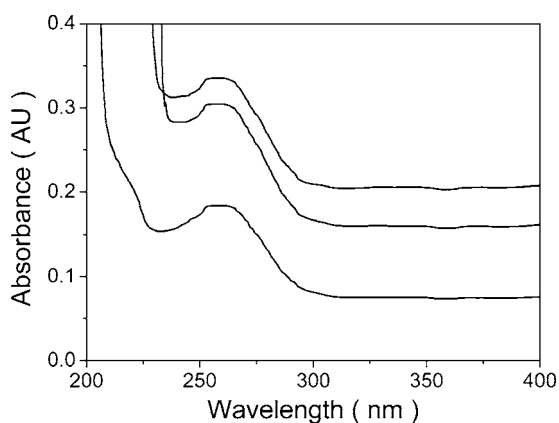
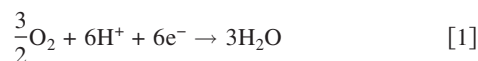


**Figure 2.** Typical UV absorption spectra showing the characteristic 258 nm peak for dissolved ozone.

diffuses into the gas diffusion cathode and combines with protons to form water when receiving electrons from the external circuit, as shown in



Ozone is generated at the anode by oxidation of water with electrons releasing to the external circuit and protons into the electrolyte, according to



The protons generated at the anode will be transported through the proton conducting polyelectrolyte Nafion membrane back to the gas diffusion cathode. The net reaction is converting oxygen to ozone without any consumption of water or protons.

A Manson SPS9400 dc power supply was used to apply a constant current or voltage to the cell. The concentration of dissolved ozone in the electrolyzed outflow was determined by the UV absorption at 258 nm measured by an AstraNet UV-visible fiber optic spectrometer with a 10 mm path length flow cell. The correlation of UV absorption intensity to ozone concentration was calculated based on a molar absorption coefficient of 2900 L/mol/cm, which was determined in other studies.<sup>20</sup> The current efficiency of ozone generation can be calculated according to Faraday's law

$$\eta = \left( \frac{nFM}{C} \right) \times 100\% \quad [3]$$

where  $n$  is the moles of electrons transferred for one mole of ozone production and is equal to 6 according to Eq 1,  $F$  is Faraday's constant and equal to 96,485 C/mol,  $M$  is the moles of ozone generated by the electrolytic cell, and  $C$  is the amount of electric charge input into the cell. The charge consumption can be calculated from the current values recorded from the power supply.

The energy consumption per unit of ozone ( $E_p$ ) was obtained as

$$E_p = (UI)/Q \quad [4]$$

where  $Q$  is the ozone production rate,  $I$  is the applied current, and  $U$  is the cell voltage reading from the dc power supply.

### Results and Discussion

**Ozone concentration and production rate.**— Steady ozone generation in water was achieved in a few minutes after water flow and electricity were turned on. Typical UV absorption curves with peaks at 258 nm, representing the characteristic peak of dissolved ozone, are shown in Fig. 2 for different online measurements. The dissolved ozone concentration estimation was based on the difference between baseline and the peak value. The absorption curves fluctuated with time due to fluctuations in water flow and occasional

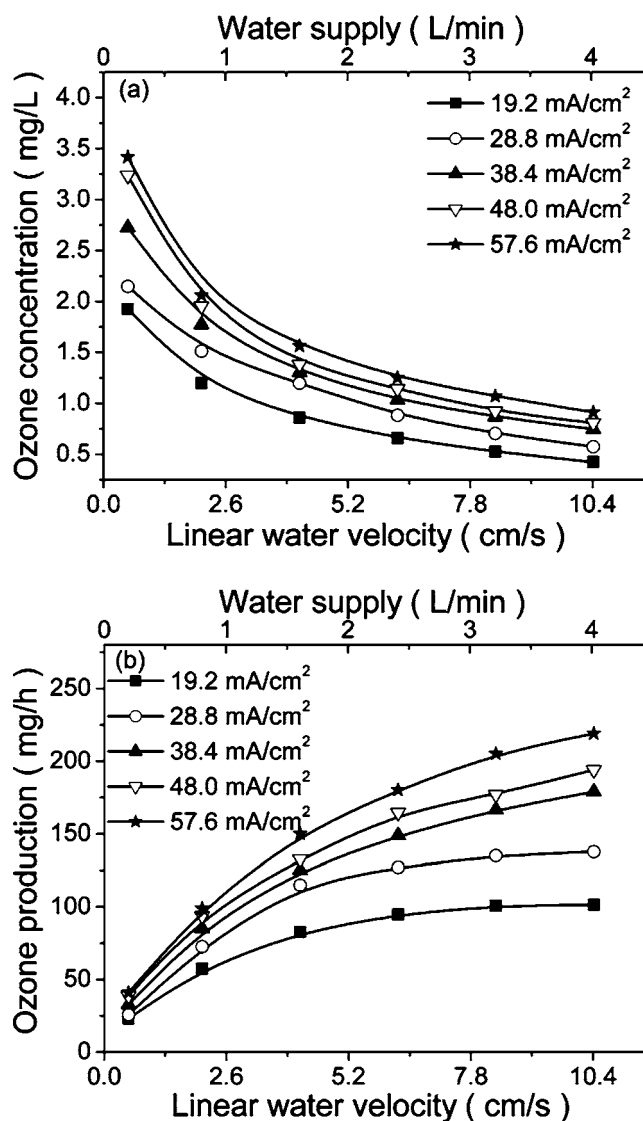


**Figure 3.** Effect of water flow on dissolved ozone concentration and ozone production rate for a single MEA at different applied currents. (a) Top panel: dissolved ozone concentration and (b) bottom panel: dissolved ozone production.

bubbles. Depending on water flow rate and ozone production, there is some ozone evolved into gas phase in the form of bubbles. The characteristic smell of ozone can be detected in the water exiting the cell, but the gaseous ozone concentration was not determined.

At steady state, the concentration of dissolved ozone depends on current input and the liquid flow rate. Ozone concentration increased with current, while an increase in flow diluted ozone in the exiting water, as shown in Fig. 3a, but the relationship is nonlinear. As anticipated, the total ozone production rate of the system increased with the current input but with a loss of current efficiency (as discussed later). At a fixed current, while a higher liquid flow reduced the ozone concentration, an increase in flow rate resulted in an overall increase in ozone production, as shown in Fig. 3b.

Ozone is an unstable chemical and decomposition to oxygen is expected. An increase in flow rate can lower concentration of dissolved ozone in the liquid and reduce the evolution rate of ozone. Water flow removes the products of electrolysis near electrode surface and improves mass transfer of electrochemical reactions. Furthermore, in the presence of bubbles due to ozone or oxygen generation, a higher flow rate with forced convection can prevent bubbles accumulation which can affect the proton transfer at anode-

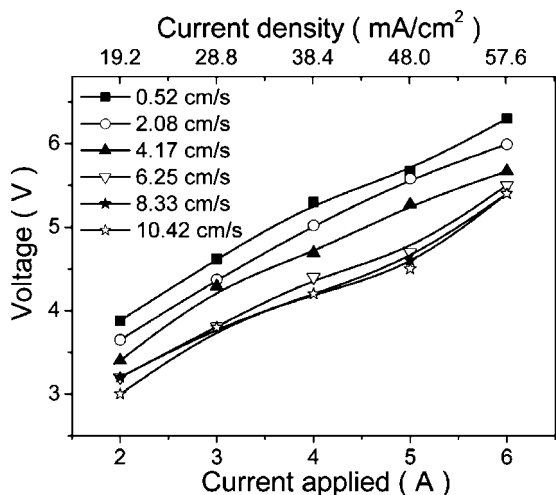


**Figure 4.** Voltage across anode and cathode vs applied current for different water flow rates past a single MEA.

Nafion interface. From Fig. 3b, the effect of flow rate on production is more evident at low flow rates, particularly at low current. It appears that mass transfer is less important at higher flow rates.

The ohmic resistance and energy efficiency can also be indirectly analyzed from the voltage developed across the cell at different currents. The variations of voltage across anode and cathode for different currents and flow rates are shown in Fig. 4. The plot of voltage vs current is quite linear but varies with flow rate. The almost parallel curves imply that the ohmic resistance across the cell is nearly the same with different flow rates, calculated to be 0.5–0.6  $\Omega$ . This is not surprising because most of the ohmic drop should be across the Nafion membrane, which is sandwiched between anode and cathode and not affected by convection. At fixed current, the voltage decreased with increasing flow rate, indicating that water convection reduces the mass-transfer resistance at the Nafion-anode-water interface and lower electrode polarization.

**Current efficiency and energy consumption.**— The current efficiency for electrochemical ozone generation varied with the current applied, and the water flow rate was shown in Fig. 5. For a given current, the current efficiency increased linearly with the flow rate, initially, but became rather constant at higher water flow rate. With

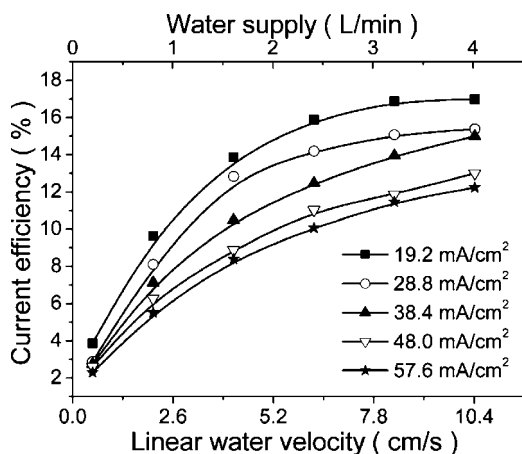


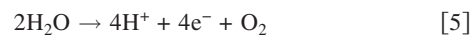
**Figure 5.** Current efficiency based on dissolved ozone production as a function of water flow and applied current for a single MEA.

**Table I.** Energy consumption for a single MEA.

Water supply (L/min)	Nom. linear water velocity (cm/s)	Current density (mA/cm <sup>2</sup> )	Energy consumption (kWh/kgO <sub>3</sub> )
0.2	0.52	19.2	336
		28.8	538
		38.4	648
		48.0	730
		57.6	922
0.8	2.08	19.2	127
		28.8	181
		38.4	236
		48.0	297
		57.6	364
1.6	4.17	19.2	82
		28.8	112
		38.4	150
		48.0	199
		57.6	227
2.4	6.25	19.2	68
		28.8	90
		38.4	118
		48.0	143
		57.6	183
3.2	8.33	19.2	63.5
		28.8	84.4
		38.4	101
		48.0	130
		57.6	158
4.0	10.42	19.2	59
		28.8	83
		38.4	94
		48.0	116
		57.6	148

the MEA tested, a steady efficiency of 17% was achieved at a current of 2 A (current density = 19.2 mA/cm<sup>2</sup>) and a flow rate of 4.0 L/min (linear velocity = 10.42 cm/s).

The loss of current efficiency is mainly due to oxygen production either directly in the electrolysis step of Eq. 5 parallel to ozone production or the subsequent decomposition of ozone to oxygen in Eq. 6



The equilibrium potential of electrolysis oxygen evolution is 1.23 V vs reference hydrogen electrode (vs RHE), which is lower than that of 1.52 V (vs RHE) for ozone generation. Hence, oxygen evolution is thermodynamically preferred to ozone production in water electrolysis. In the present study, the role of the doped SnO<sub>2</sub> at the anode surface was presumably to suppress the kinetics of oxygen evolution and promote the activation of ozone generation. Because the electrochemical kinetics of oxygen evolution and ozone generation is different, a change in voltage may have different effects on these two reactions. Though a higher ozone production is achieved by operating at 6 A (current density = 57.6 mA/cm<sup>2</sup>) (as shown in Fig. 3b), a lower efficiency is achieved compared to an applied current 2 A (current density = 19.2 mA/cm<sup>2</sup>) (as shown in Fig. 5).

The value of current efficiency was comparable to 15% reported earlier<sup>16</sup> for a smaller cell of 4 × 6 cm electrode. However, current efficiency in the earlier work was based on total ozone production including both gaseous and dissolved ozone, whereas present work only measured dissolved ozone. The current efficiency improvement on dissolved ozone production is mainly due to forced convection.

As shown in Table I, the energy consumption varied with applied current. The effect of water convection on energy efficiency is very evident. The energy consumption dramatically decreased with in-

**Table II. Ozone generation by four MEAs in the electrochemical cell.**

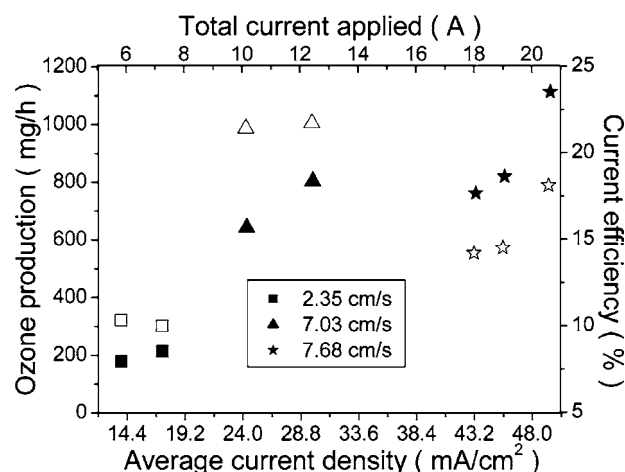
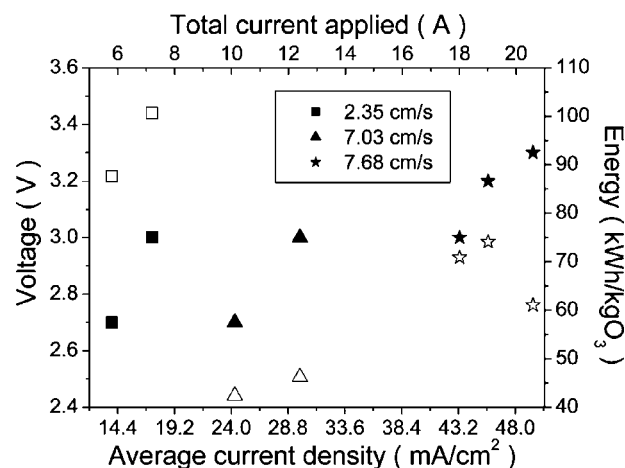
Water supply (L/min)	Total current (A)	Voltage (V)	Ozone production (mg/h)	Current efficiency (%)	Energy consumption (kWh/kgO <sub>3</sub> )	Avg. linear velocity (cm/s)	Avg. current density (mA/cm <sup>2</sup> )
1.8	5.8	~2.7	178	10.3	87.6	2.35	13.9
1.8	7.2	~3.0	214	10.0	100.7	2.35	17.3
5.4	10.1	~2.7	643	21.4	42.4	7.03	24.3
5.4	12.4	~3.0	804	21.7	46.3	7.03	29.8
5.9	18.0	~3.0	761	14.2	70.9	7.68	43.3
5.9	19.0	~3.2	820	14.5	74.1	7.68	45.7
5.9	20.6	~3.3	1113	18.1	61.1	7.68	49.5

creasing of water flow rate and >80% of energy was saved when water flow increased from 0.2 L/min (linear velocity = 0.52 cm/s) to 4 L/min (linear velocity = 10.42 cm/s). This savings was mainly due to voltage reduction as shown in Fig. 4. The lowest energy consumption of 59 kWh/kg (O<sub>3</sub>) was achieved at 2 A (current density = 19.2 mA/cm<sup>2</sup>) with a water flow rate of 4 L/min (linear velocity = 10.42 cm/s). This energy consumption is lower than that of best reported on PbO<sub>2</sub><sup>21</sup> and seems comparable to a corona discharge (CD) process if drying, cooling, and oxygen purification were all considered.<sup>3,16</sup> For producing dissolved ozone in a CD, transfer loss from gaseous ozone to aqueous ozone will lead to additional energy consumption per ozone produced.

**Multiple MEAs performance in the stack.**—The results of a single cell were based on MEA-a. Three additional MEAs (MEA-b, -c, and -d) were assembled together with MEA-a to make a stack in the configuration of Fig. 1b. The operation of a four-MEA stack was investigated. Two anodes were placed face to face sharing a common water chamber. Similarly, two face-to-face cathodes shared a common chamber with air flow. The MEA cells were connected in a parallel electric circuit with a common voltage ranging from 2.7 to 3.3 V. Anode variations led to uneven polarizations of the four MEAs and variations in current demand. The reported ozone production was the sum of the four MEAs and the current efficiency was calculated based on the total ozone production and the total current input. The nominal linear water velocity was calculated by assuming evenly distributed parallel flow into the two anode chambers.

Results of ozone generation in the four-MEA stack are given in Table II and Fig. 7 for different water flow rates. To minimize gas evolution, high current was only applied at high flow rates. As shown in Fig. 6, ozone production increased with flow rate and with current. Current efficiency is highest at 21.7% at 5.4 L/min (linear velocity = 7.03 cm/s) water flow running at 12.4 A (current density = 29.8 mA/cm<sup>2</sup>). This efficiency is higher than the results of a single MEA in Fig. 5, probably due to better performance of the three additional MEAs. Direct comparison to the single MEA results show similar results only at low flow rate and nominal velocity of 2.35 cm/s. At higher flow rates and higher total currents, there were more discrepancies between the four-MEA stack and single MEA-a, possibly due to uneven flow between the two anode chambers, uneven current distribution in the four electrodes, and uneven performance of the four MEAs. There was possible influence of mass transfer between two anodes sharing a common chamber. Table II tabulates nominal linear water velocity and average current density in the four-MEA stack. Most of the data points of stack ozone production and current efficiency are higher than those in Fig. 3b and 5, on the basis of linear water velocity and average current density. It is possible that the three additional MEAs received higher current and have better capacity on ozone generation. The highest production rate recorded was 1.1 g/h dissolved ozone with a current efficiency of 18%. The minimum energy consumption was 42 kWh/kg ozone in water. For a target application of 3 mg/L dissolved ozone, the four-MEA unit can process 367 L of water per hour.

The ozone production in a large area stack is subjected to limitations of uniform current distribution and mass transport. The present work reported reasonable results on large electrodes. There are some inherent difficulties in uniform coating of active materials on anode through the dip-coating and pyrolysis cycles, in addition to uniform pressure and heat distribution in pressing the MEA. An important aspect is maximizing the anode-Nafion interface, where ozone is generated with the simultaneous presence of protons from Nafion, water, and the anode surface. The geometry of the anode mesh, surface roughness, the amount of Nafion dispersion, tempera-

**Figure 6.** Dissolved ozone production rate (filled symbols) and corresponding current efficiency (open symbols) in a four-MEA stack.**Figure 7.** Voltage (filled symbols) and energy consumption (open symbols) with four MEAs assembled in the electrochemical cell.

ture, and pressure in MEA preparation can affect the morphology of the interface. Present results are encouraging considering further possible improvements in electrodes, MEA, and stack design.

### Conclusions

A scale-up electrochemical generation of ozone was demonstrated with pure water fed through a doped tin oxide electrode and air fed through an air diffusion cathode with electrode area  $8 \times 13$  cm. For one MEA, the rate of dissolved ozone produced was 218 mg/h at an applied current of 6 A (current density =  $57.6 \text{ mA/cm}^2$ ) with a corresponding voltage of 5.4 V across the MEA. Ozone production rate, current efficiency, and energy efficiency all increase with flow rate but level off at higher flow rates. Four MEAs in a stack gave an ozone production rate of 1.1 g/h at 20.6 A (current density =  $49.5 \text{ mA/cm}^2$ ) and 3.3 V in a parallel electrical circuit. The highest current efficiency was 21.7%, and the lowest energy consumption was 42 kWh/k ozone in water, suggesting viability of the doped tin oxide anode for ozone generation.

### Acknowledgments

This work has been financially supported by the General Research Fund of Hong Kong (grants no. HKU2006/E and no. HKU 700507P), and an Innovation Technology Seed Fund of Hong Kong (grant no. ITS/088/06). The support of Clarizon Ltd. U.K. is also acknowledged.

*University of Hong Kong assisted in meeting the publication costs of this article.*

### References

1. S. T. Oyama, *Catal. Rev. - Sci. Eng.*, **42**, 279 (2000).
2. B. Langlais, D. A. Reckhow, and D. R. Brink, *Ozone in Water Treatment Application and Engineering*, Lewis Publishers, Boca Raton (1991).
3. E. Merz and F. Gaia, *Ozone: Sci. Eng.*, **12**, 401 (1990).
4. L. M. da Silva, M. H. P. Santana, and J. F. C. Boodts, *Quim. Nova*, **26**, 880 (2003).
5. S. D. Han, J. D. Kim, K. C. Singh, and R. S. Chaudhary, *Indian J. Chem., Sect A: Inorg., Phys., Theor. Anal.*, **43**, 1599 (2004).
6. P. C. Foller and C. W. Tobias, *J. Electrochem. Soc.*, **129**, 506 (1982).
7. E. R. Kötz and S. Stucki, *J. Electroanal. Chem. Interfacial Electrochem.*, **228**, 407 (1987).
8. T. C. Wen and C. C. Chang, *J. Electrochem. Soc.*, **140**, 2764 (1993).
9. J. R. Feng, D. C. Johnson, S. N. Lowery, and J. J. Carey, *J. Electrochem. Soc.*, **141**, 2708 (1994).
10. A. A. Chernik, V. B. Drozdovich, and I. M. Zharskii, *Russ. J. Electrochem.*, **33**, 259 (1997).
11. N. Katsuki, E. Takahashi, M. Toyoda, T. Kurosu, M. Iida, S. Wakita, Y. Nishiki, and T. Shimamune, *J. Electrochem. Soc.*, **145**, 2358 (1998).
12. S. G. Park, G. S. Kim, J. E. Park, Y. Einaga, and A. Fujishima, *J. New Mater. Electrochem. Syst.*, **8**, 65 (2005).
13. K. Arihara, C. Terashima, and A. Fujishima, *J. Electrochem. Soc.*, **154**, E71 (2007).
14. S. A. Cheng and K. Y. Chan, *Electrochem. Solid-State Lett.*, **7**, D4 (2004).
15. Y. H. Wang, K. Y. Chan, S. A. Cheng, and X. Y. Li, *J. Electrochem. Soc.*, **152**, D197 (2005).
16. Y. H. Wang, K. Y. Chan, and S. A. Cheng, *Green Chem.*, **8**, 568 (2006).
17. K. Onda, T. Ohba, H. Kusunoki, S. Takezawa, D. Sunakawa, and T. Araki, *J. Electrochem. Soc.*, **152**, D177 (2005).
18. J. Kim and G. V. Korshin, *Ozone: Sci. Eng.*, **30**, 113 (2008).
19. X. Y. Li, Y. H. Cui, Y. J. Feng, Z. M. Xie, and J. D. Gu, *Water Res.*, **39**, 1972 (2005).
20. J. Hoigné and H. Bader, *Water Res.*, **10**, 377 (1976).
21. S. Stucki, H. Baumann, H. J. Christen, and R. Kötz, *J. Appl. Electrochem.*, **17**, 773 (1987).